Crystal Structure of the *Neisseria gonorrhoeae* MtrD Inner Membrane Multidrug Efflux Pump

Jani Reddy Bolla[1][9], Chih-Chia Su[2][9], Sylvia V. Do[3][9], Abhijith Radhakrishnan[1], Nitin Kumar[1], Feng Long[2], Tsung-Han Chou[2], Jared A. Delmar[2], Hsiang-Ting Lei[1], Kanagalaghatta R. Rajashankar[4], William M. Shafer[5][6], Edward W. Yu[1][2][3]*

1 Department of Chemistry, Iowa State University, Ames, Iowa, United States of America, 2 Department of Physics and Astronomy, Iowa State University, Ames, Iowa, United States of America, 3 Bioinformatics and Computational Biology Interdepartmental Graduate Program, Iowa State University, Ames, Iowa, United States of America, 4 NE-CAT and Department of Chemistry and Chemical Biology, Cornell University, Argonne National Laboratory, Argonne, Illinois, United States of America, 5 Department of Microbiology and Immunology, Emory University School of Medicine, Atlanta, Georgia, United States of America, 6 Laboratories of Microbial Pathogenesis, VA Medical Center, Decatur, Georgia, United States of America

Abstract

Neisseria gonorrhoeae is an obligate human pathogen and the causative agent of the sexually-transmitted disease gonorrhea. The control of this disease has been compromised by the increasing proportion of infections due to antibiotic-resistant strains, which are growing at an alarming rate. The MtrCDE tripartite multidrug efflux pump, belonging to the hydrophobic and amphiphilic efflux resistance-nodulation-cell division (HAE-RND) family, spans both the inner and outer membranes of *N. gonorrhoeae* and confers resistance to a variety of antibiotics and toxic compounds. We here report the crystal structure of the inner membrane MtrD multidrug efflux pump, which reveals a novel structural feature that is not found in other RND efflux pumps.

Competing Interests: The authors have declared that no competing interests exist.

* E-mail: ewyu@iastate.edu

[9] These authors contributed equally to this work.

Introduction

Neisseria gonorrhoeae is a Gram-negative obligate human pathogen. It is the causative agent of the sexually-transmitted disease gonorrhea and rare cases of disseminated disease. Although gonorrhea is one of the oldest described diseases, it remains a significant global problem with more than 100 million cases reported annually worldwide and antibiotic resistance is a major concern [1]. The gonococcus employs a number of strategies to evade host attack. It possesses an intricate mechanism of antigenic variability through differential expression of the genome and can easily acquire new genetic material to develop resistance to antimicrobial agents [1,2]. Gonococci utilize a number of resistance mechanisms, including antimicrobial inactivation, target modification and strategies that reduce antimicrobial concentration, such as reduced permeability of the cell envelope mediated through alteration of porin proteins and active export of multiple antimicrobial compounds from the cell by efflux pumps. Among these different mechanisms, multidrug efflux is considered to be one of the major causes of failure of drug-based treatments of infectious diseases, which appears to be increasing in prevalence [3]. These bacterial multidrug efflux pumps have enormous clinical consequences. Simultaneously rendering the cell resistant to multiple structurally-unrelated compounds, their expression results in bacterial strains resistant to most clinically-relevant antibiotics [3].

The best characterized and most clinically important of these multidrug efflux systems in *N. gonorrhoeae* is the MtrCDE tripartite efflux pump [4–7]. It is composed of the MtrD inner membrane transporter, belonging to the HAE-RND protein family [8]; the MtrC periplasmic protein, a member of the membrane fusion protein family; and the MtrE integral outer membrane channel protein. This system provides resistance to a broad spectrum of antimicrobial agents, including bile salts, fatty acids, dyes, antibiotics and spermicides. The Mtr multidrug efflux system is also responsible for resistance to host-derived cationic antimicrobial peptides [7], which are important mediators of the innate host defense. Given that gonococci commonly infect mucosal sites bathed in fluids containing such peptides, the Mtr system indeed underscores the pathogenesis of gonococcal disease and its contribution to virulence. In addition, it has been shown that the MtrCDE tripartite efflux pump is capable of enhancing long-term colonization of the mouse vaginal mucosal layer and that gonococci lacking this efflux pump were highly attenuated [9].

At present, only two crystal structures of HAE-RND-type efflux pumps are available. These efflux pumps are the *Escherichia coli*

AcrB [10–18] and *Pseudomonas aeruginosa* MexB [19] multidrug transporters. Their structures suggest that both AcrB and MexB span the entire width of the inner membrane and protrude approximately 70 Å into the periplasm. Along with the models of these two HAE-RND transporters, the crystal structures of the other components of these tripartite complex systems have also been determined. These include the outer membrane channels *E. coli* TolC [20] and *P. aeruginosa* OprM [21], as well as the periplasmic membrane fusion proteins *E. coli* AcrA [22] and *P. aeruginosa* MexA [23–25].

Currently, no structural information is available for any protein component of the MtrCDE tripartite complex system. To elucidate the mechanism used by this efflux system for multidrug recognition and extrusion, we here describe the crystal structure of the inner membrane MtrD multidrug efflux pump. The findings reveal a novel structural feature that is not found in other known RND efflux pumps.

Results and Discussion

Overall Structure of the *N. gonorrhoeae* MtrD Multidrug Efflux Pump

We cloned, expressed and purified the full-length MtrD efflux pump containing a 6xHis tag at the C-terminus. We obtained crystals of this membrane protein following an extensive screening for crystallization conditions with different detergents. We then used molecular replacement, utilizing the structure of the "access" protomer of AcrB (pdb code: 2DHH) [12] to determine the three-dimensional structure. The diffraction data can be indexed to the space group *R*32. Data collection and refinement statistics are summarized in Table 1. The resulting electron density maps (Fig. 1) reveal that the asymmetric unit consists of one protomer. The crystal structure of the MtrD multidrug efflux pump has been determined to a resolution of 3.53 Å (Table 1). Currently, 97% of the amino acids (residues 2–493 and 508–1040) are included in the final model (Fig. 2a). The final structure is refined to R_{work} and R_{free} of 27.9% and 33.3%, respectively. The structure of MtrD is closer to the conformation of the "access" protomer of AcrB. However, superimposition of these two structures results in a high RMSD of 7.6 Å over 1,000 C^{α} atoms, suggesting that there are significant differences between these two transporters (Fig. S1).

MtrD assembles as a 125-Å long and 95-Å wide homotrimer (Fig. 2b). Each protomer comprises 12 transmembrane helices (TM1–TM12). Like other RND transporters, the N-terminal (TM1–TM6) and C-terminal (TM7–TM12) halves of MtrD are related by a pseudo-twofold symmetry. A large periplasmic domain is created by two extensive periplasmic loops connecting TM1 with TM2 and TM7 with TM8, respectively. As in AcrB [10–18] and MexB [19], this periplasmic domain can be divided into six sub-domains: PN1, PN2, PC1, PC2, DN and DC (Figs. 2 and 3). Sub-domains PN1, PN2, PC1 and PC2 form the pore domain, with PN1 making up the central pore and stabilizing the trimeric organization. However, sub-domains DN and DC contribute to form the docking domain, presumably interacting with the outer membrane channel MtrE. The trimeric MtrD structure suggests that sub-domains PN2, PC1 and PC2 are located at the outermost core of the periplasmic domain, facing the periplasm. Sub-domains PC1 and PC2 also form an external cleft, and this cleft is open in the MtrD structure (Fig. 2). Based on the co-crystal structure of CusBA [26,27] of the CusCBA tripartite efflux system [28–33], the upper regions of PN2, PC1, PC2 and sub-domains DN and DC should directly interact with the MtrC membrane fusion protein to form a functional adaptor-transporter complex.

The *N. gonorrhoeae* MtrCDE tripartite efflux system has the advantage that all these protein components are encoded by the same operon. Thus, the interactions between different proteins are likely to be specific, facilitating analyses of how different components function cooperatively.

Periplasmic Multidrug Binding Site

Crystallization of AcrB with a variety of substrates [12,16–18] has identified that the periplasmic cleft of the pump forms several mini-binding pockets within the extensive, large periplasmic multidrug binding site. This site is supposed to play a predominant role in the selection of drugs for export. Protein sequence alignment reveals that many of the amino acids forming the large periplasmic binding site of AcrB are conserved among MexB and MtrD, indicating that these three multidrug efflux pumps may have a similar substrate binding profile for drug recognition. These conserved amino acids in MtrD include several charged and polar residues, such as S79, S134, R174, D272, E669 and R714, and aromatic residues, such as F136, F176, F610, F612 and F623 (Fig. 3).

A flexible loop is found inside the large periplasmic cleft (Fig. S1), which form the multidrug binding site of the pump. This flexible loop is located deep inside the cleft between subdomains PC1 and PC2, composed of residues 608–619, and should correspond to the Phe-617 loop [16] in AcrB. The loop is highly conserved among MtrD, AcrB and MexB. It is expected that this flexible loop is important for drug recognition and extrusion. There is a chance that this loop may shift positions during the course of the extrusion process to facilitate drug export.

Transmembrane Helix TM9

Perhaps the most interesting secondary structural feature appears in TM9 of the MtrD pump. In contrast to other known structures of the RND transporters, MtrD contains an extended region that protrudes into the periplasm and contributes part of the periplasmic domain (Figs. 2 and 3). This region (residues 917–927) comprises an α-helix extending from the upper portion of TM9 and also to the loop connecting TM9 and TM10. Protein sequence alignment suggests that these extra residues are only found in MtrD and not other homologous RND proteins. Therefore, this fragment should represent a unique feature of this pump that cannot be found in other RND pumps. TM9 is distinct in that it is not vertically oriented. Instead, it is inclined from the horizontal membrane plane by 54°. The spatial arrangement between the extra elongated helix and loop (upper portion of TM9) and the periplasmic cleft formed between PC1 and PC2 suggests that these extra structural features may help the pump to transport its substrates more effectively from the outer leaflet of the inner membrane to the multidrug binding site at the periplasmic domain (Fig. 4).

Proton-relay Network

Drug export by RND transporters is proton motive force (PMF)-dependent. Based on the crystal structure of MtrD, it is expected that the charged residues D405 and D406 of TM4 and K948 of TM10 are important for forming the proton-relay network of the pump (Fig. 5). These residues are supposed to undergo protonation and deprotonation within the transport cycle. The involvement of these charged amino acids in proton translocation was supported by a previous study that showed mutations of these residues inhibits proton translocation [34]. In turn, the MtrE outer membrane channel protein is blocked and unable to dissociate from the MtrCDE tripartite efflux complex [34].
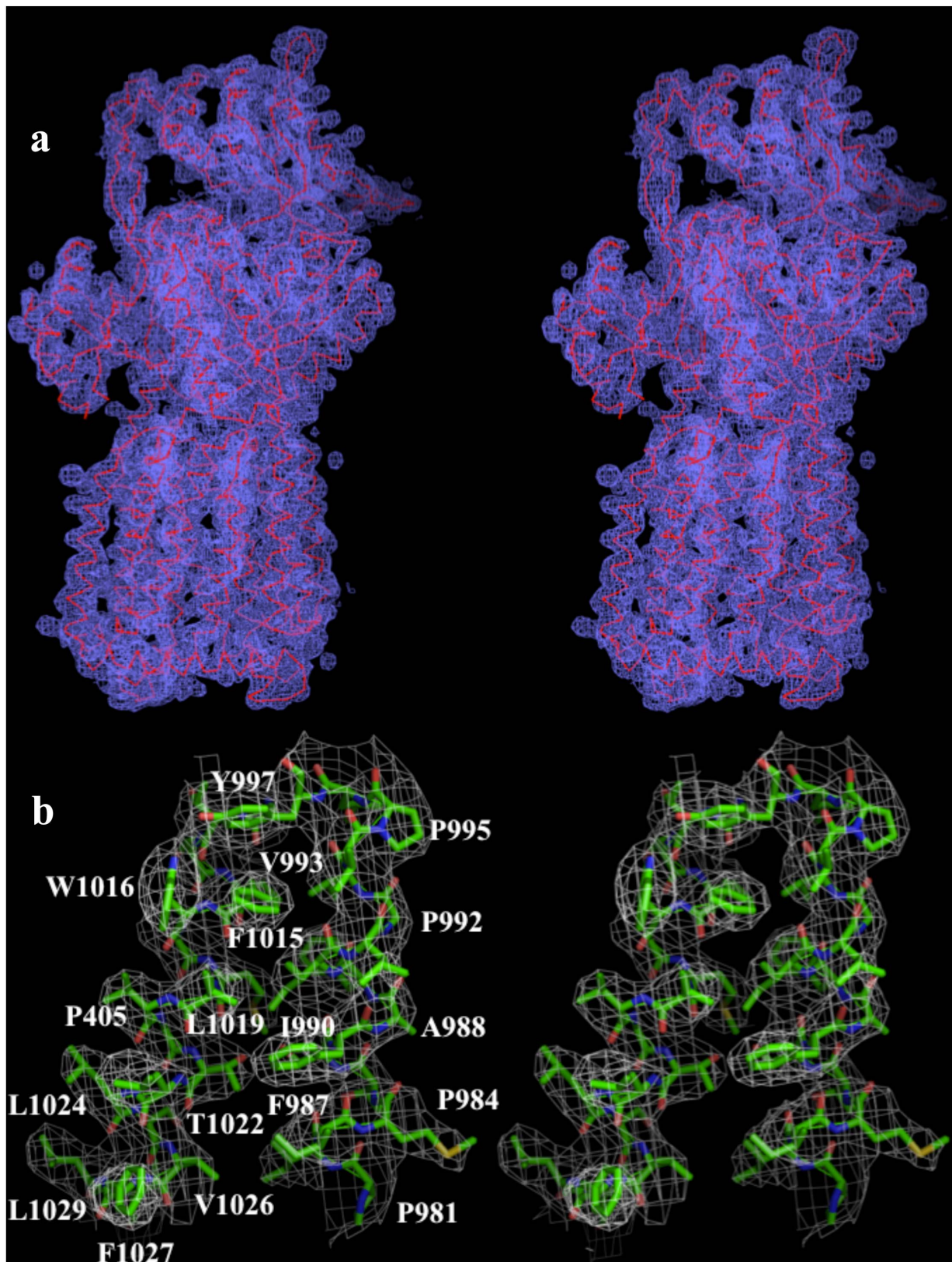
Figure 1. Stereo view of the electron density map of the MtrD efflux pump at a resolution of 3.53 Å. (a) The electron density map contoured at 1.2 σ is in blue. The Cα traces of MtrD are in red. (b) Representative section of the electron density at the interface between TM11 and TM12 of MtrD. The electron density (colored white) is contoured at the 1.2 σ level and superimposed with the final refined model (green, carbon; red, oxygen; blue, nitrogen).

Table 1. Data collection and refinement statistics.

Data set	MtrD
Data Collection	
Wavelength (Å)	0.98
Space group	*R*32
Resolution (Å)	50–3.53
	(3.68–3.53)
Cell constants (Å)	
a	152.99
b	152.95
c	360.74
α, β, γ (°)	90, 90, 120
Molecules in ASU	1
Redundancy	2.9 (2.9)
Total reflections	377,955
Unique reflections	20,296
Completeness (%)	97.7 (98.0)
R_{sym} (%)	7.7 (42.9)
$I/\sigma(I)$	17.16 (1.9)
Refinement	
Resolution (Å)	50–3.53
R_{work}	27.9
R_{free}	33.3
rms deviation from ideal	
bond lengths (Å)	0.003
bond angles (°)	0.794
Ramachandran	
most favoured (%)	89.6
additional allowed (%)	10.1
generously allowed (%)	0.3
disallowed (%)	0

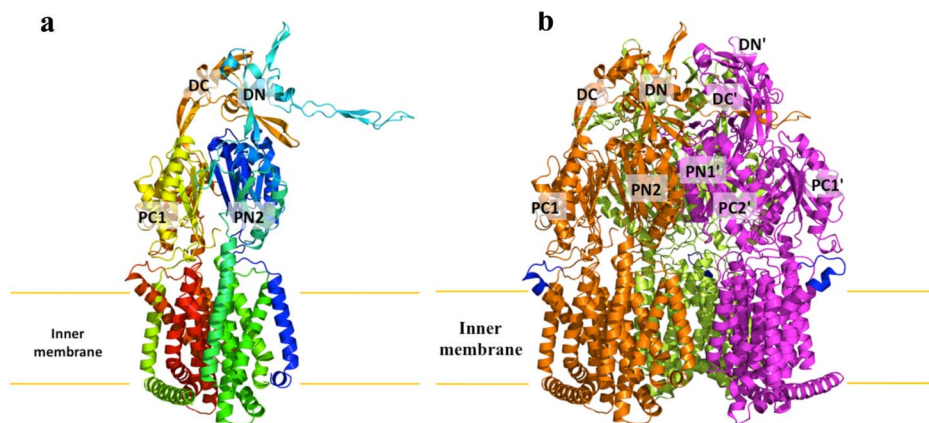doi:10.1371/journal.pone.0097903.t001

Figure 2. Structure of the *N. gonorrhoeae* MtrD efflux pump. (a) Ribbon diagram of a protomer of MtrD viewed in the membrane plane. The molecule is colored using a rainbow gradient from the N-terminus (blue) to the C-terminus (red). Sub-domains DN, DC, PN2, PC1 and PC2 are labeled. The location of PN1 is behind PN2, PC1 and PC2. (b) Ribbon diagram of the MtrD trimer viewed in the membrane plane. Each subunit of MtrD is labeled with a different color. Residues 917–927 (only found in MtrD) forming the upper portion of TM9 and the loop connecting TM9 and TM10 are in blue color.
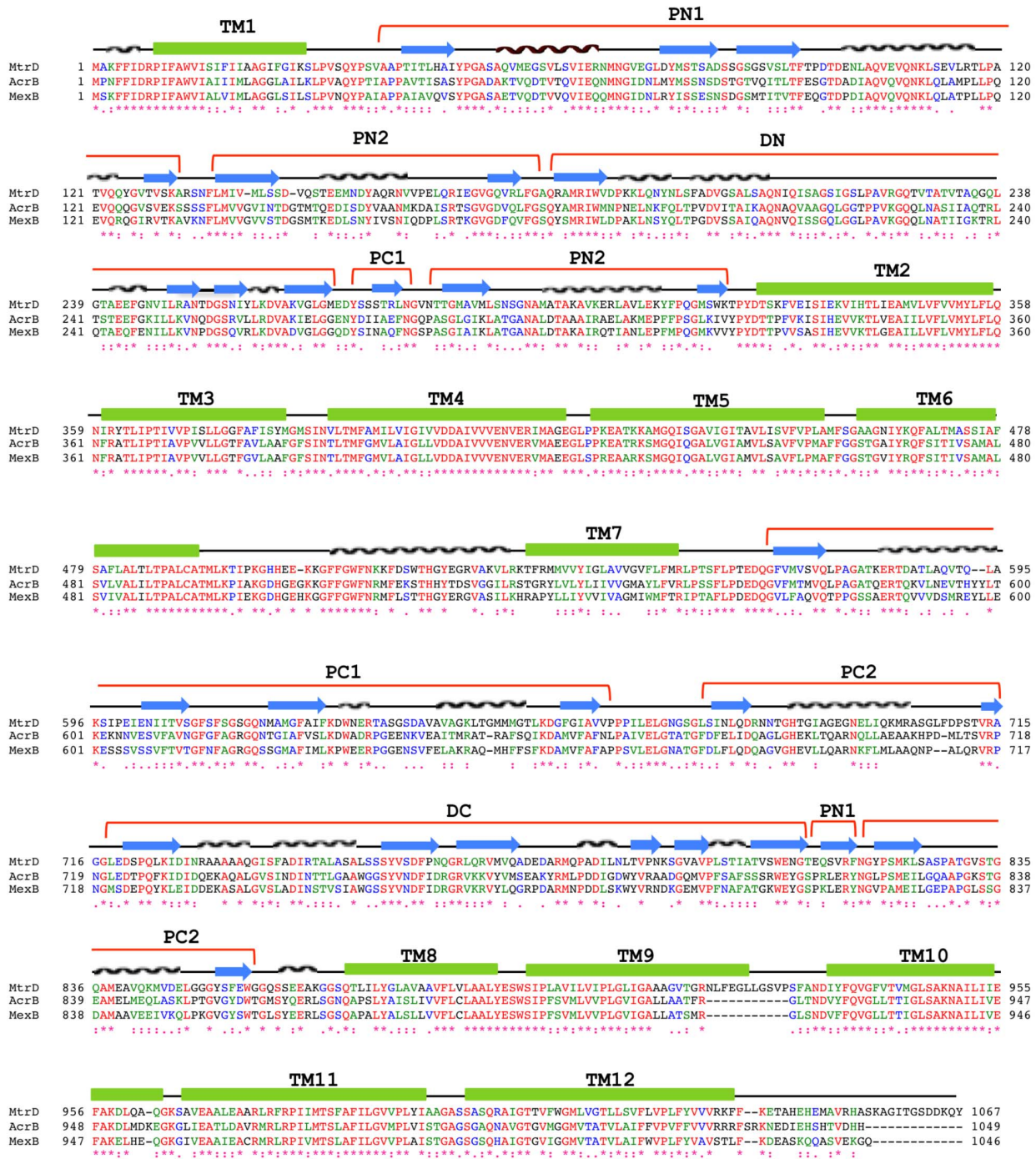doi:10.1371/journal.pone.0097903.g002

Figure 3. Sequence and topology of MtrD, AcrB and MexB. Alignment of the amino acid sequences of MtrD, AcrB and MexB were done using CLUSTAL W (*, identical residues; :, >60% homologous residues). Secondary structural elements are indicated: TM, transmembrane helix; Nα and Nβ, helix and strand, respectively, in the N-terminal half; Cα and Cβ, helix and strand, respectively, in the C-terminal half. The MtrE docking domain is divided into two sub-domains, DN and DC; whereas the pore domain is divided into four sub-domains, PN1, PN2, PC1 and PC2. The sequence and topology of MtrD are shown at the top.
doi:10.1371/journal.pone.0097903.g003

The MtrD multidrug efflux pump should operate through an alternating-access mechanism, similar to the AcrB transporter. Thus, the pump has to go through the transport cycle, which should involve different transient conformations, including the "access", "binding" and "extrusion" states of this protein. In the MtrD trimer, the conformations of the three protomers are identical to each other, suggesting that these protomers represent the same transient state. In comparison with the structures of AcrB, the conformation of MtrD is closer to that of the "access" protomer of AcrB (Fig. S1). Therefore, our MtrD structure should represent the "access" transient state of the pump. It is expected that this pump will change in conformation to go through the
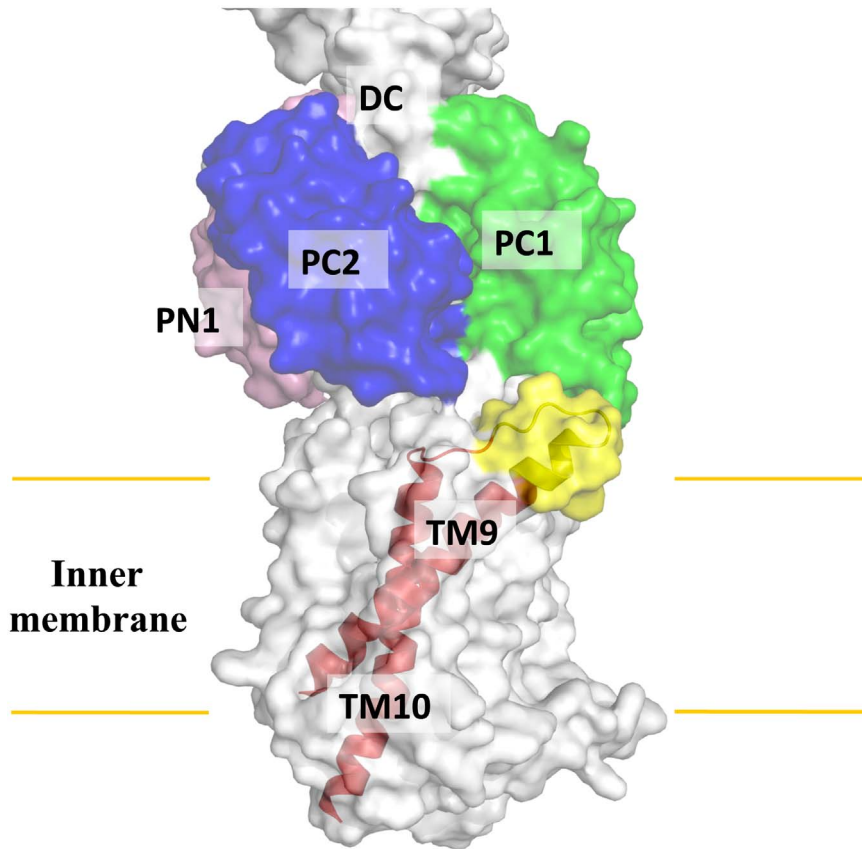
Figure 4. Spatial arrangement between TM9 and the periplasmic cleft. TM9 is inclined from the horizontal membrane plane by 54°. The extra feature (yellow), which is only found in the MtrD pump within the family, is located right next the cleft formed by subdomains PC1 and PC2.
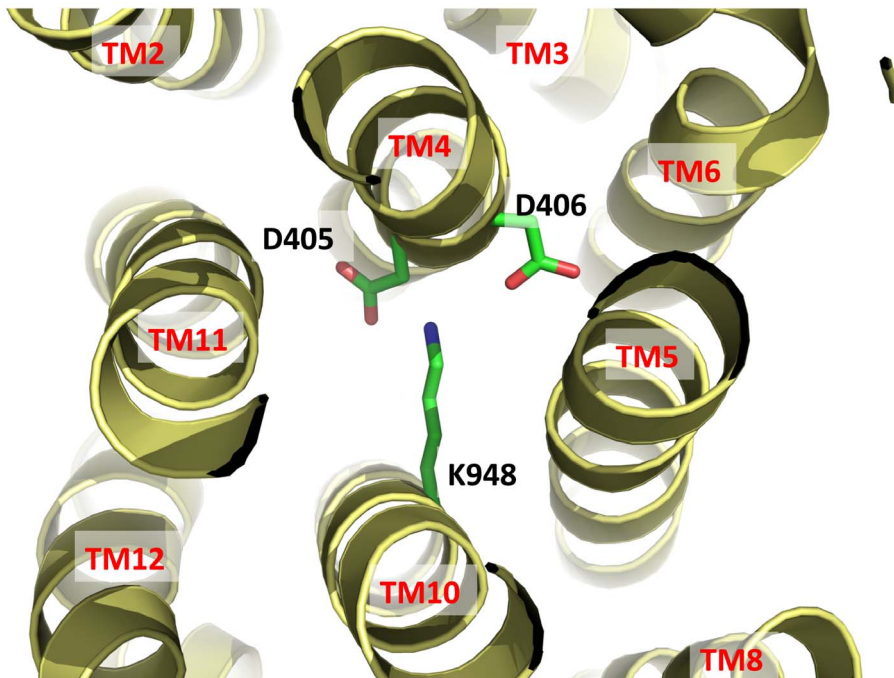doi:10.1371/journal.pone.0097903.g004

Figure 5. Ion pairs in the transmembrane domain viewed from the cytoplasmic side. Residues D405 and D406 of TM4 and K948 of TM10 that form ion pairs, which may play an important role in proton translocation, are in green sticks.
doi:10.1371/journal.pone.0097903.g005

cycle. This conformational change should be coupled to the PMF initiated by the proton-relay network.

Methods

Cloning, Expression and Purification of the Inner Membrane MtrD Efflux Pump

Briefly, the full-length MtrD membrane protein containing a 6xHis tag at the C-terminus was overproduced in *E. coli* C43(DE3)*ΔacrB* cells, which harbor a deletion in the chromosomal *acrB* gene, possessing pET15bΩ*mtrD*. Cells were grown in 12 L of 2xYT medium with 100 µg/ml ampicillin at 25°C. When the OD_{600} reached 0.6, the culture was treated with 1 mM IPTG to induce *mtrD* expression, and cells were harvested within 15 h. The collected bacteria were resuspended in low salt buffer containing 100 mM sodium phosphate (pH 7.2), 10% glycerol, 1 mM ethylenediaminetetraacetic acid (EDTA) and 1 mM phenylmethanesulfonyl fluoride (PMSF), and then disrupted with a French pressure cell. The membrane fraction was collected and washed twice with high salt buffer containing 20 mM sodium phosphate (pH 7.2), 2 M KCl, 10% glycerol, 1 mM EDTA and 1 mM PMSF, and once with 20 mM HEPES-NaOH buffer (pH 7.5) containing 1 mM PMSF. The membrane protein was then solubilized in 2% (w/v) 6-cyclohexyl-1-hexyl-β-D-maltoside (Cymal-6). Insoluble material was removed by ultracentrifugation at 100,000×g. The extracted protein was purified with a Ni^{2+}-affinity column. The purity of the MtrD protein (>95%) was judged using 10% SDS-PAGE stained with Coomassie Brilliant Blue. The purified protein was then dialyzed and concentrated to 20 mg/ml in a buffer containing 20 mM Na-HEPES (pH 7.5) and 0.05% Cymal-6.

Crystallization of MtrD

Crystals of the 6xHis MtrD were obtained using sitting-drop vapor diffusion. The MtrD crystals were grown at room temperature in 24-well plates with the following procedures. A 2 µl protein solution containing 20 mg/ml MtrD protein in 20 mM Na-HEPES (pH 7.5) and 0.05% (w/v) Cymal-6 was mixed with a 2 µl of reservoir solution containing 30% PEG 400, 0.1 M Na-Bicine (pH 8.5), 0.1 M NH_4Cl, 0.05 M $BaCl_2$ and 9% glycerol. The resultant mixture was equilibrated against 500 µl of the reservoir solution. Crystals of MtrD grew to a full size in the drops within a week. Typically, the dimensions of the crystals were 0.2 mm×0.2 mm×0.2 mm. The crystals were flash-cooled, using solution containing 40% PEG 400, 0.1 M Na-Bicine (pH 8.5), 0.1 M NH_4Cl, 0.05 M $BaCl_2$, 9% glycerol and 0.05% Cymal-6 as a cryoprotectant before data collection.

Data Collection, Structural Determination and Refinement

All diffraction data were collected at 100 K at beamline 24ID-C located at the Advanced Photon Source, using an ADSC Quantum 315 CCD-based detector. Diffraction data were processed using DENZO and scaled using SCALEPACK [35].

Crystals of the MtrD efflux pump belong to the space group *R*32 (Table 1) and the best crystal diffracted x-ray to a resolution of 3.53 Å. Analysis of Matthew's coefficient indicated the presence of one MtrD protomer (113.69 kDa) per asymmetric unit, with a solvent content of 66.7%.

The structure of MtrD was phased using molecular replacement, utilizing the structure of the "access" protomer of AcrB (pdb id: 2DHH) [12] as a search model. After tracing the initial model manually using the program Coot [36], the model was refined against the native data at 3.53 Å-resolution using TLS refinement techniques adopting a single TLS body as implemented in PHENIX [37] leaving 5% of reflections in Free-R set. Iterations of refinement using PHENIX [37] and CNS [38] and model building in Coot [36] lead to the current model, which consists of 1,025 residues with excellent geometrical characteristics (Table 1).

Accession Code

Atomic coordinates and structure factors have been deposited in the Protein Data Bank with accession code 4MT1.

Supporting Information

Figure S1 Comparison of the structures of the MtrD and AcrB efflux pumps. (a) Ribbon diagram of protomers of MtrD and AcrB viewed in the membrane plane. This is a superimposition of a subunit of MtrD (red) onto an "access" protomer of AcrB (pdb: 2DHH) (green), indicating that the structures of these two efflux pumps are quite distinct. Superimposition of these two structures result in a high RMSDs of 7.6 Å over 1,000 C^{α} atoms. (b) Front view of the periplasmic clefts, formed by subdomains PC1 and PC2, of MtrD and AcrB. The secondary structural elements of these two transporters are colored red (MtrD) and green (AcrB). (c) Potential multidrug binding within the periplasmic cleft of MtrD. The flexible loop created by residues 608–619 is colored blue. This loop should correspond to the Phe-617 loop in AcrB. It is suspected that this flexible loop may swing into this drug binding site to facilitate export during drug extrusion. The rest of the secondary structural elements of MtrD are colored red.
(TIF)

Author Contributions

Conceived and designed the experiments: JRB CS SVD EWY. Performed the experiments: JRB CS SVD AR NK FL TC JAD HL. Analyzed the data: JRB CS SVD KRR EWY. Contributed reagents/materials/analysis tools: JRB CS SVD AR NK FL TC JAD HL. Wrote the paper: JRB CS SVD WMS EWY.

References

1. Tapsall J (2006) Antibiotic resistance in *Neisseria gonorrhoeae* is diminishing available treatment options for gonorrhea: some possible remedies. Expert Review of Anti-infective Therapy 4: 619–628.
2. Stern A, Brown M, Nickel P, Meyer TF (1986) Opacity genes in *Neisseria gonorrhoeae*: Control of phase and antigenic variation. Cell 47: 61–71.
3. Piddock LJ (2006) Multidrug-resistance efflux pumps? not just for resistance. Clin Microbiol Rev 19: 382–402.
4. Warner DM, Shafer WM, Jerse AE (2008) Clinically relevant mutations that cause derepression of the *Neisseria gonorrhoeae* MtrC-MtrD-MtrE efflux pump system confer different levels of antimicrobial resistance and *in vivo* fitness. Mol Microbiol 70: 462–478.
5. Hagman KE, Lucas CE, Balthazar JT, Snyder LA, Nilles M, et al. (1997) The MtrD protein of *Neisseria gonorrhoeae* is a member of resistance/nodulation/division protein family constituting part of an efflux system. Microbiology 143: 2117–2125.
6. Lucas CE, Hagman KE, Levin JC, Stein DC, Shafer WM (1995) Importance of lipooligosaccharide structure in determining gonococcal resistance to hydrophobic antimicrobial agents resulting from the *mtr* efflux system. Mol Microbiol 16: 1001–1009.
7. Shafer WM, Qu XD, Waring AJ, Lehrer RI (1998) Modulation of *Neisseria gonorrhoeae* susceptibility to vertebrate antibacterial peptides due to a member of the resistance/nodulation/division efflux pump family. Proc Natl Acad Sci USA 95: 1829–1833.

8. Tseng TT, Gratwick KS, Kollman J, Park D, Nies DH, et al. (1999) The RND permease superfamily: an ancient, ubiquitous and diverse family that includes human disease and development protein. J Mol Microbiol Biotechnol 1: 107–125.

9. Jerse AE, Sharma ND, Simms AN, Crow ET, Snyder LA, et al. (2003) A gonococcal efflux pump system enhances bacterial survival in a female mouse model of genital tract infection. Infection and Immunity 71: 5576–5582.

10. Murakami S, Nakashima R, Yamashita E, Yamaguchi A (2002) Crystal structure of bacterial multidrug efflux transporter AcrB. Nature 419: 587–593.

11. Yu EW, McDermott G, Zgurskaya HI, Nikaido H, Koshland DE Jr (2003) Structural basis of multiple drug binding capacity of the AcrB multidrug efflux pump. Science 300: 976–980.

12. Murakami S, Nakashima R, Yamashita E, Matsumoto T, Yamaguchi A (2006) Crystal structures of a multidrug transporter reveal a functionally rotating mechanism. Nature 443: 173–179.

13. Seeger MA, Schiefner A, Eicher T, Verrey F, Dietrichs K, et al. (2006) Structural asymmetry of AcrB trimer suggests a peristaltic pump mechanism. Science 313: 1295–1298.

14. Sennhauser G, Amstutz P, Briand C, Storchenegger O, Grütter MG (2007) Drug export pathway of multidrug exporter AcrB revealed by DARPin inhibitors. PLoS Biol 5: e7.

15. Yu EW, Aires JR, McDermott G, Nikaido H (2005) A periplasmic-drug binding site of the AcrB multidrug efflux pump: a crystallographic and site-directed mutagenesis study. J Bacteriol 187: 6804–6815.

16. Nakashima R, Sakurai K, Yamasaki S, Nishino K, Yamaguchi A (2011) Structures of the multidrug exporter AcrB reveal a proximal multisite drug-binding pocket. Nature 480: 565–569.

17. Nakashima R, Sakurai K, Yamasaki S, Hayashi K, Nagata C, et al. (2013). Structural basis for the inhibition of bacterial multidrug exporters. Nature 500: 102–106.

18. Eicher T, Cha H, Seeger MA, Brandstätter L, El-Delik J, et al. (2012) Transport of drugs by the multidrug transporter AcrB involves an access and a deep binding pocket that are separated by a switch-loop. Proc Natl Acad Sci USA 109: 5687–5692.

19. Sennhauser G, Bukowska MA, Briand C, Grütter MG (2009) Crystal structure of the multidrug exporter MexB from *Pseudomonas aeruginosa*. J Mol Biol 389: 134–145.

20. Koronakis V, Sharff A, Koronakis E, Luisi B, Hughes C (2000) Crystal structure of the bacterial membrane protein TolC central to multidrug efflux and protein export. Nature 405: 914–919.

21. Akama H, Kanemaki M, Yoshimura M, Tsukihara T, Kashiwag T, et al. (2004) Crystal structure of the drug discharge outer membrane protein, OprM, of *Pseudomonas aeruginosa*. J Biol Chem 279: 52816–52819.

22. Mikolosko J, Bobyk K, Zgurskaya HI, Ghosh P (2006) Conformational flexibility in the multidrug efflux system protein AcrA. Structure 14: 577–587.

23. Higgins MK, Bokma E, Koronakis E, Hughes C, Koronakis V (2004) Structure of the periplasmic component of a bacterial drug efflux pump. Proc Natl Acad Sci USA 101: 9994–9999.

24. Akama H, Matsuura T, Kashiwag S, Yoneyama H, Narita S, et al. (2004) Crystal structure of the membrane fusion protein, MexA, of the multidrug transporter in *Pseudomonas aeruginosa*. J Biol Chem 279: 25939–25942.

25. Symmons M, Bokma E, Koronakis E, Hughes C, Koronakis V (2009) The assembled structure of a complete tripartite bacterial multidrug efflux pump. Proc Natl Acad Sci USA 106: 7173–7178.

26. Su CC, Long F, Lei HT, Bolla JR, Do SV, et al. (2012) Charged amino acids (R83, E567, D617, E625, R669, and K678) of CusA are required for metal ion transport in the Cus efflux system. J Mol Biol 422: 429–441.

27. Su CC, Long F, Zimmermann MT, Rajashankar KR, Jernigan RL, et al. (2011) Crystal Structure of the CusBA Heavy-Metal Efflux Complex of *Escherichia coli*. Nature 470: 558–562.

28. Long F, Su CC, Zimmermann MT, Boyken SE, Rajashankar KR, et al. (2010) Crystal structures of the CusA heavy-metal efflux pump suggest methionine-mediated metal transport mechanism. Nature 467: 484–488.

29. Su CC, Yang F, Long F, Reyon D, Routh MD, et al. (2009) Crystal structure of the membrane fusion protein CusB from *Escherichia coli*. J Mol Biol 393: 342–355.

30. Kulathila R, Kulathila R, Indic M, van den Berg B (2011) Crystal structure of *Escherichia coli* CusC, the outer membrane component of a heavy-metal efflux pump. PLoS One 6: e15610.

31. Lei HT, Bolla JR, Bishop NR, Su CC, Yu EW (2014) Crystal structures of CusC review conformational changes accompanying folding and transmembrane channel formation. J Mol Biol 426: 403–411.

32. Franke S, Grass G, Nies DH (2001) The product of the *ybdE* gene of the *Escherichia coli* chromosome is involved in detoxification of silver ions. Microbiology 147: 965–972.

33. Franke S, Grass G, Rensing C, Nies DH (2003) Molecular analysis of the copper-transporting efflux system CusCFBA of *Escherichia coli*. J Bacteriol 185: 3804–3812.

34. Janganan TK, Bavro VN, Zhang L, Borges-Walmsley MI, Walmsley AR (2013) Tripartite efflux pumps: energy is required for dissociation, but not assembly or opening of the outer membrane channel of the pump. Mol Microbiol 88: 590–602.

35. Otwinowski Z, Minor M (1997) Processing of X-ray diffraction data collected in oscillation mode. Methods Enzymol 276: 307–326.

36. Emsley P, Cowtan K (2004) Coot: model-building tools for molecular graphics. Acta Crystallogr D 60: 2126.

37. Adams PD, Grosse-Kunstleve RW, Hung LW, Ioerger TR, McCroy AJ, et al. (2002) PHENIX: building new software for automated crystallographic structure determination. Acta Crystallogr D 58: 1948–1954.

38. Brünger AT, Adams PD, Clore GM, DeLano WL, Gros P, et al. (1998) Crystallography & NMR system: A new software suite for macromolecular structure determination. Acta Crystallogr D 54: 905–921.